twin boundaries (Fig. 5), and from electron microscope observations and diffraction patterns. Electron microscopy (*3*) has shown the twin planes to be parallel (110) planes. We interpret the rows of image spots as images of atoms or molecules because they are sometimes single spots, as from a typical metal specimen, and sometimes doublet spots, as seen in FIM images of molecular species (*15*). In the present images, the doublet spots could be images of metal oxides. We associate the layer-imaging phase with the orthorhombic (superconducting) structure based on the earlier diffraction work on similar material. The other prevalent phase (Fig. 3B), which gave relatively disordered images, we associate with the nonsuperconducting tetragonal structure for similar reasons. We have found both phases in both types of material studied, but the "as prepared" samples were predominantly of the orthorhombic phase.

Since we have not yet performed atom probe mass analysis (*14*) to identify the preferentially imaging atomic or molecular species of the superconducting phase, we can only surmise, guided by computer-simulated field ion images, which atoms or molecules comprise the imaged layers. Computer simulations similar to those used in interpreting FIM images of alloys (*16*) were made to compare with the present micrographs, based on the orthorhombic unit cell of $YBa_2Cu_3O_{7-x}$ (*5*) (Fig. 6). Only those images due to the Cu-O end planes and possibly images due to only the yttrium atoms appear to be similar to the actual FIM images.

Both the superconducting and nonsuperconducting phases would be expected on the basis of atomic structure (*4, 9*) to image similarly in the FIM, unless the occurrence of superconductivity caused some selective phenomenon in the imaging process. Only the superconducting phase of $YBa_2Cu_3O_{7-x}$ appeared to field evaporate as though it was composed of layers of atoms with a relatively lower work function or higher binding energy, separated by more easily field evaporated atoms. Alternatively, the FIM image was consistent with a material composed of conducting layers separated by (nonimaging) insulating spaces. We have obtained similar results for the high T_c superconductor $YbBa_2Cu_3O_{7-x}$.

We performed experiments in which the superconducting phase was raised to about 100 K or to 300 K (both above T_c) and then re-recooled to 25 to 40 K. If no imaging was done during the time the specimen was at the higher temperatures, the preferentially imaged layers were always again seen at the low temperature. Attempts to observe a superconducting-to-normal transition by FIM, however, were not decisive (poor image quality at high temperature) due possibly to gaseous impurities in the unbaked microscope. At temperatures above T_c, the images consisted of a brightly imaging disordered array of spots and some barely discernible parallel rows. The strongly layered image, characteristic of the superconducting phase, did not always reappear when the recooling was done while continuously imaging in hydrogen. This result could be due to excessive depletion of oxygen from the specimens. Field electron microscopy (FEEM) images of the superconducting phase were observed also, but these were subject to rapid contamination in the poor vacuum ($\sim 5 \times 10^{-7}$ Pa).

We conclude that FIM and FEEM studies of the high T_c superconducting ceramics are feasible and can be used to provide detailed information about local structural and electronic properties of the various phases and their interfaces (such as phase boundaries, grain boundaries, and defects) in these fascinating materials. Although there are still some questions about the detailed interpretation of our results, the present work has provided a real space correlation between the FIM images and the occurrence of the superconducting phase in $YBa_2Cu_3O_{7-x}$ and $YbBa_2Cu_3O_{7-x}$. The observations of selectively imaging layers in the superconducting material possibly imply that the superconductivity is, in fact, inhomogeneous on an atomic scale and localized to specific layers. We tentatively identify these layers as the (Cu-O) end planes of the orthorhombic unit cell in single crystals of $YBa_2Cu_3O_{7-x}$ and $YbBa_2Cu_3O_{7-x}$.

REFERENCES AND NOTES

1. G. Bednorz and K. A. Muller, *Z. Phys.* **64**, 189 (1986); C. W. Chu *et al.*, *Phys. Rev. Lett.* **58**, 405 (1987).
2. R. Wagner, *Field-Ion Microscopy in Materials Science*, vol. 6 of Crystals Series (Springer-Verlag, Berlin, 1982).
3. G. Van Tendeloo, H. W. Zandbergen, S. Amelinckx, *Solid State Commun.* **63**, 389 (1987).
4. R. J. Cava *et al.*, *Phys. Rev. Lett.* **58**, 1676 (1987).
5. F. Beech, S. Miraglia, A. Santoro, R. S. Roth, *Phys. Rev. B* **35**, 8778 (1987).
6. T. Siegrist, S. Sunshine, D. W. Murphy, R. J. Cava, S. M. Zahurak, *ibid.*, p. 7137.
7. J. M. Tarascon, W. R. McKinnon, L. H. Greene, G. W. Hull, E. M. Vogel, *ibid.* **36**, 226 (1987).
8. J. Marcus *et al.*, *Solid State Commun.* **63**, 129 (1987).
9. M. P. Maple *et al.*, *ibid.*, p. 635.
10. A. Santoro *et al.*, *Mater. Res. Bull.* **22**, 1007 (1987).
11. Y. Hidaka, Y. Enomoto, M. Suzuki, M. Oda, J. Murakami, *Jpn. J. Appl. Phys. Part 2* **26**, L377 (1987).
12. T. R. Dinger, T. K. Worthington, W. J. Gallagher, R. L. Sandstrom, *Phys. Rev. Lett.* **58**, 2687 (1987).
13. H. Noel *et al.*, *Solid State Commun.* **63**, 915 (1987).
14. E. W. Müller and T. T. Tsong, *Field Ion Microscopy Principles and Applications* (Elsevier, New York, 1969).
15. A. J. Melmed, in *Field Ion Microscopy*, J. J. Hren and S. Ranganathan, Eds. (Plenum, New York, 1968), p. 183.
16. A. J. W. Moore, *ibid.*, p. 69.

17. We thank L. A. Bendersky for transmission electron microscopy work and J. Blendell and A. L. Johnson for providing some sample material.

29 October 1987; accepted 25 November 1987

Role of the Protein Moiety of Ribonuclease P, a Ribonucleoprotein Enzyme

CLAUDIA REICH, GARY J. OLSEN, BERNADETTE PACE, NORMAN R. PACE

The *Bacillus subtilis* ribonuclease P consists of a protein and an RNA. At high ionic strength the reaction is protein-independent; the RNA alone is capable of cleaving precursor transfer RNA, but the turnover is slow. Kinetic analyses show that high salt concentrations facilitate substrate binding in the absence of the protein, probably by decreasing the repulsion between the polyanionic enzyme and substrate RNAs, and also slow product release and enzyme turnover. It is proposed that the ribonuclease P protein, which is small and basic, provides a local pool of counter-ions that facilitates substrate binding without interfering with rapid product release.

RIBONUCLEASE P (RNASE P) removes 5′ sequences from precursor transfer RNAs (pre-tRNAs). The enzymes from the eubacteria *Escherichia coli* and *Bacillus subtilis* (*1*) are ribonucleoproteins (RNPs) consisting of an RNA (400 nucleotides) (*2, 3*) and a protein (14 kD) (*4*). Although RNase P functions in vivo as an RNP, under certain conditions the RNA alone is capable of binding and precisely cleaving tRNA precursors (*5*). We undertook a kinetic study of the RNase P reaction in *B. subtilis* to elucidate the role of the protein moiety in an RNP.

Under physiological ionic conditions, both the RNA and protein components of RNase P are required for catalysis. The

Department of Biology and Institute for Molecular and Cellular Biology, Indiana University, Bloomington, IN 47405.

requirement for the protein moiety is alleviated by high concentrations of mono- and divalent cations (*5*). To assess whether this effect is exerted during substrate binding, the catalytic process, or both, we evaluated the effect of ionic strength and RNase P protein on the kinetic parameters K_m and k_{cat} for the cleavage of pre-tRNA by RNase P RNA (Fig. 1). Double-reciprocal (Lineweaver-Burk) plots of RNase P RNA activity as a function of substrate concentration, under different ionic conditions, show that an increase in the concentration of mono- and divalent cations causes a decrease in the Michaelis constant, K_m (Fig. 2A); the binding efficiency is enhanced. The overall catalytic rate (k_{cat}) is essentially the same under all these conditions, implying that the salt does not induce a transition from a less active to a more active conformation of the RNase P RNA.

In a comparison of the RNA-alone reaction, under optimal ionic conditions, with that of the holoenzyme, the K_m values are essentially the same (Fig. 2B), indicating that both bind the substrate comparably; the RNase P protein and high ionic strength have the same influence on the RNase P RNA during substrate binding. The nonspecific nature of a high ionic strength solution suggests an electrostatic role for the positively charged (*4*) RNase P protein as well. However, the protein has an influence not mimicked by salt; the k_{cat} of the holoenzyme is approximately 20 times greater than that of the RNA-alone reaction (Fig. 2B).

The enhancement of the catalytic rate by the protein could be accomplished in several ways: The protein could participate in the mechanism of the reaction, for example, by providing catalytically active groups; it could accelerate the rate of cleavage of the phosphodiester bond by facilitating binding of the substrate; or it might allow rapid dissociation of the enzyme-product complex after cleavage, increasing the rate of turnover. To elucidate the role of the RNase P protein in pre-tRNA processing, initial reaction rates were analyzed at a ratio of substrate to enzyme of 2 to 1. This allowed us to compare the first round of substrate binding and cleavage in the RNA-alone and the holoenzyme reactions. The influence of product release on the activity was tested by loading the enzyme with product (mature tRNA) prior to the addition of substrate (pre-tRNA); slow product release would delay the first round of cleavage relative to that observed upon the simultaneous addition of product and substrate.

Initiating the RNase P RNA–alone reaction by mixing enzyme and substrate RNAs (E + S) at high salt concentrations results in a rapid first round of cleavage (Fig. 3A). About half of the substrate is cleaved during this initial burst, an amount stoichiometric with the enzyme. The initial burst is nearly complete after 15 seconds, and the amount of rapid cleavage is proportional to the concentration of RNase P RNA (Fig. 4). The amount of substrate cleaved during the first minute in the reaction with RNA alone (Fig. 3A) is greater than the extent of reaction carried out by the same amount of holoenzyme in the same period (Fig. 3B). Thus, the stimulation of the overall velocity (k_{cat}) by the protein (Fig. 2B) cannot be at the steps of binding or cleaving the substrate.

When RNase P RNA–alone reactions are initiated with a mixture of precursor and mature tRNA (Fig. 3A; E + [S + I]), the initial burst of pre-tRNA cleavage is reduced by a factor of 4, consistent with the corresponding dilution of the substrate by mature tRNA, a competitive inhibitor of both the RNA-alone and holoenzyme reactions. During binding, RNase P does not discriminate between precursor and mature tRNAs; the recognition sites for the enzyme lie within the mature tRNA domain. This has been shown in genetic analyses with bacteriophage T4 tRNAs (*6*) and is supported by kinetic analyses (*7*). However, when the enzyme RNA is loaded with mature tRNA prior to the addition of pre-tRNA substrate, the initial burst of cleavage disappears (Fig. 3A; [E + I] + S). This indicates that mature tRNA does not dissociate readily from the enzyme-RNA surface after cleavage, preventing the access of further substrate molecules. In contrast, the early holoenzyme reaction is not preferentially inhibited by mature tRNA, and varying the order of addition of substrate and inhibitor has no effect on the extent of inhibition. Thus, the

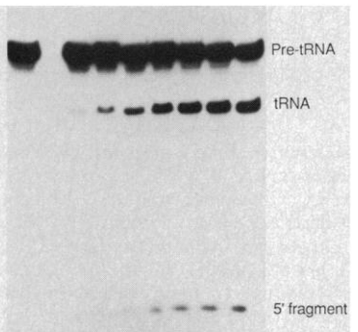

Fig. 1. RNase P activity assay. Activity was assayed at 37°C by incubating uniformly ^{32}P-labeled pre-tRNA^{Asp} with RNase P RNA alone or in the presence of saturating amounts of purified RNase P protein (holoenzyme). Substrate and enzyme RNAs were produced by in vitro transcription of the corresponding genes cloned adjacent to T_7 promoters in appropriate expression vectors (*3*). RNA-alone reactions were carried out in 50 m*M* tris-HCl, *p*H 8.0, 0.05% NP40, and concentrations of NH_4Cl and $MgCl_2$ as indicated. Holoenzyme reactions were carried out in 50 m*M* tris-HCl, *p*H 8.0, 100 m*M* NH_4Cl, 15 m*M* $MgCl_2$. Reactions were stopped by adding three volumes of cold ethanol, and products were resolved on 8% polyacrylamide gels containing 8*M* urea. After fixing and drying the gels, the product bands were located by autoradiography, excised, and counted. The autoradiograph shows the time course for the cleavage of pre-tRNA^{Asp} by RNase P RNA that had been preincubated with mature tRNA. Sampling times were, from left to right, 0, 1, 3, 5, 10, 15, 20, and 30 minutes. The results of this assay are plotted as "(E + I) + S" in Fig. 3B.

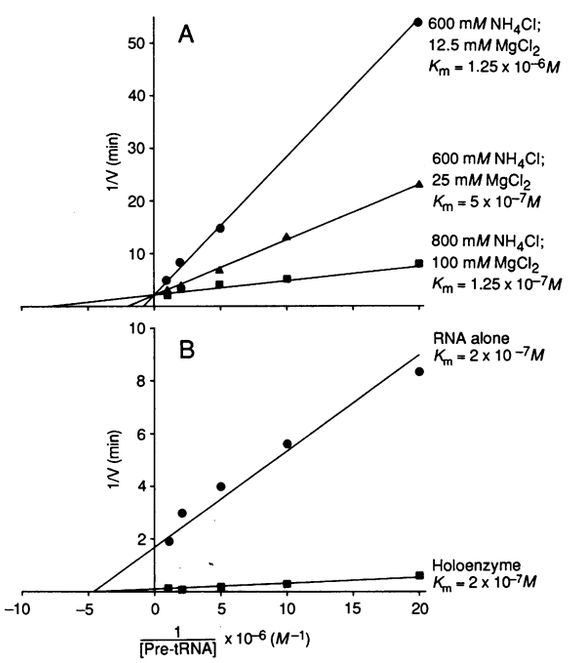

Fig. 2. Kinetic analysis of the RNase P reaction under various conditions. (**A**) Double-reciprocal (Lineweaver-Burk) plot of RNase P RNA activity as a function of substrate concentration. (**B**) Double-reciprocal plot of RNase P RNA and holoenzyme activities as a function of substrate concentration. Ionic conditions were optimal for both reactions, namely, 800 m*M* NH_4Cl, 100 m*M* $MgCl_2$ for RNA alone and 100 m*M* NH_4Cl, 15 m*M* $MgCl_2$ for holoenzyme. Enzyme concentrations were $7.5 \times 10^{-9}M$ and $1.5 \times 10^{-9}M$ for the RNA-alone and holoenzyme reactions, respectively. Reaction rates are expressed as moles of substrate cleaved per mole of enzyme per minute.

rate of dissociation of the cleaved product from the holoenzyme is rapid compared to the rate of release from the RNase P RNA alone.

In summary, either high ionic strength or the RNase P protein are required for RNase P RNA to cleave pre-tRNAs. As the salt concentration is raised, the affinity of RNase P RNA for its substrate (as reflected in K_m) increases (Fig. 2A). At optimal (high) salt concentrations, RNase P RNA has a K_m for pre-tRNA comparable to that of the holoenzyme at moderate ionic strength; however, its cleavage rate (k_{cat}) is approximately 20 times lower than that of the holoenzyme (Fig. 2B). Order of addition experiments (Fig. 3) indicate that in the RNA-alone reaction at high ionic strength (i) the first round of substrate cleavage is more rapid than subsequent rounds, (ii) pre-tRNA and mature tRNA compete for enzyme during the first round of binding and cleavage, and (iii) bound tRNA is slow to dissociate upon addition of pre-tRNA. In the holoenzyme reaction, which occurs at relatively low ionic strength, there is no obvious distinction between the first and subsequent rounds of cleavage.

These data suggest a qualitative model (Fig. 5) for the role of the RNase P protein. Anionic repulsion between enzyme and substrate RNAs must be screened to allow binding and catalysis; either high ionic strength or the RNase P protein can accomplish this. However, there is more rapid dissociation of the product from the holoenzyme. The RNase P protein is basic and small compared to the RNA and might provide only a localized titration of the enzyme and substrate (or product) phosphates at physiological ionic strength. Some of the repulsion between the two RNAs would remain, driving product dissociation. The high salt concentrations required to manifest the RNA-alone activity would nonspecifically titrate the phosphates of both RNAs, decreasing intermolecular repulsion and increasing the residence time of the product on the enzyme surface. The example of RNase P suggests that electrostatic insulation may be a common role of proteins in other RNP complexes, for instance, small nuclear RNPs in RNA splicing, or in the ribosome. Such proteins would constitute local pools of counterions to neutralize charge repulsion between polynucleotides under cellular conditions.

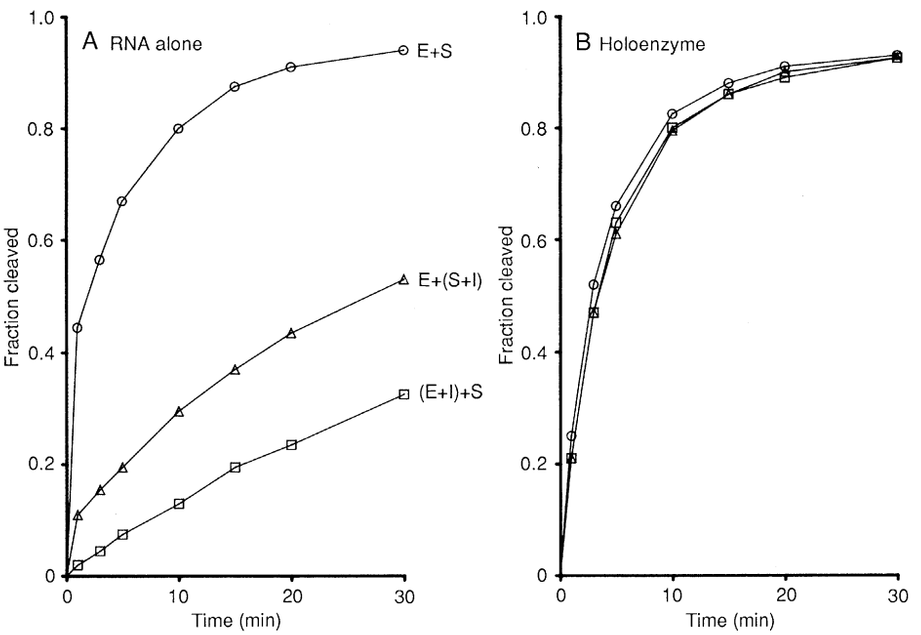

Fig. 3. Early course of the RNase P reaction in the presence or absence of mature tRNA competitor. Pre-tRNA^{Asp} (S), inhibitor bulk tRNA (I), and either RNase P RNA or holoenzyme (E) were preincubated in reaction conditions for 15 minutes at 37°C, either alone or in the combinations shown in parentheses. Reactions were initiated by combining either enzyme and substrate (E + S), or enzyme and substrate plus tRNA (E + [S + I]), or enzyme plus tRNA and substrate ([E + I] + S). RNA-alone reactions were carried out in 50 m*M* tris-HCl, *p*H 8.0, 0.05% NP40, 2*M* NH_4Cl, 100 m*M* $MgCl_2$ (to accentuate the binding effect, the salt concentrations were higher than those that maximize the net rate of catalysis). Holoenzyme reactions were carried out in 50 m*M* tris-HCl, *p*H 8.0, 100 m*M* NH_4Cl, 15 m*M* $MgCl_2$. Concentrations of reactants were [S], $3 \times 10^{-8}M$; [E], $1.5 \times 10^{-8}M$; and [I], $10^{-7}M$. At the indicated times, portions were removed and precipitated with ethanol. The extent of the reaction was determined as described in Fig. 1 and is reported as the fraction of substrate cleaved. (**A**) RNA-alone reactions. (**B**) Holoenzyme reactions.

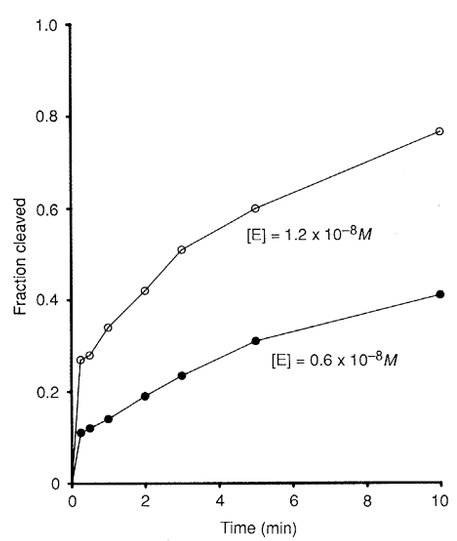

Fig. 4. Early course of the RNase P RNA–alone reaction at different concentrations of RNA enzyme. Reactions were carried out at 2*M* NH_4Cl, 100 m*M* $MgCl_2$. At the indicated times, portions were removed and the extent of reaction was determined. Concentration of substrate was $3 \times 10^{-8}M$.

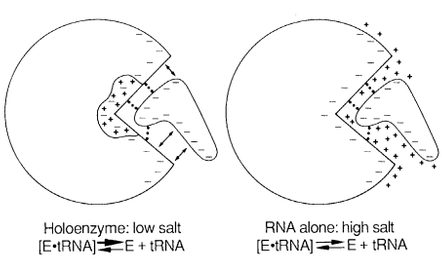

Fig. 5. Schematic representation of the influence of salt and RNase P protein on the RNA-catalyzed reaction. The plus symbol (+) indicates positively charged residues in the RNase P protein (left) or inorganic cations (right). The RNase P protein titrates local anionic repulsion in the RNA enzyme so that the pre-tRNA substrate may bind. Because the protein provides only localized charge titration, intrinsic repulsion between the RNAs remains, driving dissociation of the product after cleavage. In the RNA-alone reaction, high ionic strength screens the anionic repulsion in a generalized manner, and product dissociation is impeded.

REFERENCES AND NOTES

1. B. C. Stark, R. Kole, E. J. Bowman, S. Altman, *Proc. Natl. Acad. Sci. U.S.A.* **74**, 3717 (1978); K. Gardiner and N. R. Pace, *J. Biol. Chem.* **255**, 7507 (1980).
2. R. E. Reed, M. Baer, C. Guerrier-Takada, H. Donis-Keller, S. Altman, *Cell* **30**, 627 (1982); H. Sakamoto, N. Kimura, F. Nagawa, Y. Shimura, *Nucleic Acids Res.* **11**, 8237 (1983).
3. C. Reich *et al.*, *J. Biol. Chem.* **261**, 7888 (1986).
4. N. Ogasawara, S. Moriya, K. von Meyenburg, F. Hansen, H. Yoshikawa, *EMBO J.* **4**, 3345 (1985). The molecular sizes and net charges of the RNase P proteins (13.8 kD for *E. coli* and 14.1 kD for *B. subtilis*) were deduced from the nucleotide sequence of the *rnpA* gene region in *E. coli* and a structurally homologous open-reading frame in *B. subtilis*.

5. C. Guerrier-Takada, K. Gardiner, T. L. Marsh, N. R. Pace, S. Altman, *Cell* **35**, 849 (1983); K. J. Gardiner, T. L. Marsh, N. R. Pace, *J. Biol. Chem.* **255**, 7507 (1985).
6. G. P. Mazzara and W. H. McClain, in *Transfer RNA: Biological Aspects*, D. Söll, J. Abelson, P. Schimmel, Eds. (Cold Spring Harbor Laboratory, Cold Spring Harbor, NY, 1980), pp. 3–27.
7. C. Reich, unpublished results.
8. Supported by NIH grant GM34527 (N.R.P.).

20 July 1987; accepted 23 November 1987

Anti-Idiotypic Network Induced by T Cell Vaccination Against Experimental Autoimmune Encephalomyelitis

OFER LIDER, TAMARA RESHEF, EVELYNE BERAUD, AVRAHAM BEN-NUN, IRUN R. COHEN

In a study of the mechanism of resistance to autoimmune disease induced by T cell vaccination, rats were vaccinated against experimental autoimmune encephalomyelitis (EAE) by injecting them once in the hind footpads with a subencephalitogenic dose (10^4) of a clone of T lymphocytes specific for myelin basic protein (BP). The response to vaccination was assayed by challenging the rats with an encephalitogenic dose (3×10^6) of T lymphocytes of this BP-specific clone. Five to six days after vaccination, the cells responsible for mediating resistance to adoptively transferred EAE were concentrated in the popliteal lymph nodes draining the vaccination site. Transfer of the draining lymph node cells to unvaccinated rats led to loss of resistance in the donor rats and acquisition of resistance by the recipient rats. Limiting-dilution cultures of the draining lymph node cells were established with irradiated cells of the BP-specific clone as stimulators. Two sets of T lymphocytes specifically responsive to the BP-specific T cells from the clone were isolated: $CD4^+CD8^-$ helper and $CD4^-CD8^+$ suppressor cells. The helper T cells, like the BP antigen, specifically stimulated the BP-specific vaccinating clone. In contrast, the suppressor T cells specifically suppressed the response of the BP-specific vaccinating clone to its BP antigen. These results suggest that T cell vaccination induces resistance to autoimmune disease by activating an anti-idiotypic network.

WE HAVE INDUCED RESISTANCE to various experimental autoimmune diseases by vaccinating rats or mice with autoimmune T lymphocytes of the antigen specificity relevant to the particular disease (*1–4*). Our strategy for studying and manipulating autoimmune disease experimentally has been to isolate, in culture, lines and clones of T lymphocytes functionally active in producing experimental autoimmune encephalomyelitis (EAE), experimental autoimmune thyroiditis, or adjuvant arthritis (*4–7*). These T cells have been useful in investigating factors in pathogenesis such as the identity of critical self-epitopes (*8, 9*), traffic of autoimmune T lymphocytes through blood vessels to target organs (*10, 11*), and interactions between autoimmune T lymphocytes and target tissues (*12, 13*). Autoimmune T lymphocytes, in addition to probing pathogenesis, can be rendered avirulent and used to induce resistance to the specific autoimmune disease with which they are associated. We have called this practice T cell vaccination by its analogy to the use of attenuated agents of infectious disease for similar ends (*2*).

At first, we used irradiated autoimmune effector T cells for vaccination (*2*). Recently we found vaccination to be more effective when we used T cells treated by hydrostatic pressure or chemical cross-linkers (*14, 15*). However, some untreated autoimmune effector clones can also be used as vaccine if a dose of cells below the threshold number needed for disease is administered (*4, 16*). Common to all forms of vaccination is the requirement that the T cells be activated, prior to inoculation, by incubation with specific antigen or a T cell mitogen such as concanavalin A together with antigen-presenting cells (*10*). T cell vaccination induced lasting remission of established autoimmune disease and prevented the development of subsequent induction of disease (*15*).

The strategy in the present study was to vaccinate rats in the hind footpads with cells of a T cell clone specifically directed against myelin basic protein (anti-BP T cells) and to assay the draining popliteal lymph node (PLN) and a distal lymph node for the presence of cells able to recognize the anti-BP T cells and to mediate resistance to adoptive EAE. We used the anti-BP T cells designated Z1a, which was isolated in 1980 (*17*). Recent analysis of the T cell receptor gene rearrangements of Z1a indicates that it is a single clone (*18*). Clone Z1a is reactive to an epitope within the encephalitogenic peptide (amino acids 68–88) of myelin basic protein (*9*). Z1a regularly produces EAE when injected intravenously at doses of 10^5 cells or greater, but induces resistance to EAE without first causing either clinical EAE or histologic lesions of EAE when injected at doses of 10^3 to 10^4 cells (*16*).

Table 1 shows the results of an experiment in which Lewis rats were vaccinated in the hind footpads with 10^4 mitogen-activated Z1a T cells. At various times the draining PLN and distal cervical lymph nodes (CLN) were assayed for T cell proliferative responses to the Z1a clone or to control clone A2b. [A2b is a helper T cell clone that responds to *Mycobacterium tuberculosis* and to joint cartilage (*8*) and can be used as a potent vaccine against adjuvant arthritis, but not against EAE (*15*).] Before vaccination and 2 days after vaccination, the rats showed background proliferative responses in PLN and CLN populations to both Z1a and A2b clones. However, on day 5 after vaccination (and also on day 6 in other experiments), the PLN, but not the CLN, showed a specific response to vaccinating clone Z1a. By day 11 (and also on day 9 in other experiments), the response had become systemic and both PLN and CLN populations responded to Z1a specifically.

To learn whether the response to Z1a was associated with protection against EAE, we transferred the responding PLN cells from vaccinated to naïve rats. In the experiment shown in Table 2, Lewis rats were vaccinated in the hind footpads and 6 days later the draining PLN of some rats were excised. The PLN cells were activated by a mitogen and transferred intraperitoneally into naïve recipient rats. Control rats either were not vaccinated or were inoculated with the mitogen-activated PLN cells of unvaccinated rats. One day later all the rats (unvaccinated controls, PLN donors, and PLN recipients) were tested for susceptibility to EAE produced by intravenous inoculation of 3×10^6 Z1a cells. All of the 17 control rats (unvaccinated or recipients of PLN of unvaccinated rats) developed EAE, fatal in 14 of 17 animals (the sum of the numbers of animals in groups 1, 2, and 5). In contrast, none of the 15 vaccinated rats with intact PLN developed EAE (group 3). Thus vaccination with 10^4 Z1a cells was markedly effective ($P < 0.02$, with Bonferroni correction).

O. Lider, T. Reshef, A. Ben-Nun, I. R. Cohen, Department of Cell Biology, Weizmann Institute of Science, Rehovot 76100, Israel.
E. Beraud, Laboratoire d'Immunopathologie, Université d'Aix-Marseille, 13385 Marseille, Cedex 5, France.